JOURNAL OF
Materials
CHEMISTRY

High frequency EPR of europium(II)-doped strontium aluminate phosphors

T. Nakamura,*[a] K. Kaiya,[b] N. Takahashi,[a] T. Matsuzawa,[c] C. C. Rowlands,[d] (the late) V. Beltran-Lopez,[e] G. M. Smith[f] and P. C. Riedi[f]

[a]*Department of Materials Science & Technology, Faculty of Engineering, Shizuoka University, Hamamatsu 432, Japan. E-mail: tctnaka@ipc.shizuoka.ac.jp; Fax: +81 53 478 1156; Tel: +81 53 478 1156*
[b]*Graduate School of Science and Technology, Shizuoka University, Shizuoka University, Hamamatsu 432-8561, Japan*
[c]*R & D Center, Nemoto & Company Ltd, 4-10-9 Takaido-higashi, Suginami, Tokyo, 168, Japan*
[d]*National EPSRC ENDOR Centre, Department of Chemistry, Cardiff University, P.O. Box 912, Cardiff, CF1 3TB*
[e]*Instituto de Ciencias Nucleares, Universidad Nacional Autonoma de Mexico, Ciudad Universitaria, Mexico D. F., Mexico*
[f]*School of Physics & Astronomy, University of St. Andrews, North Haugh, St. Andrews, Fife, UK KY16 9SS*

Received 22nd May 2000, Accepted 2nd August 2000

The europium(II) sites in $Sr_4Al_{14}O_{25}$: Eu phosphor with blue emission were examined by means of high frequency (90 and 180 GHz) EPR spectroscopy. The ions occupy two low symmetry sites in the $Sr_4Al_{14}O_{25}$ lattice with $|D| = 0.100$ and $0.0907\ cm^{-1}$ respectively; the ratio $|E/D|$ is estimated to be 1/3 regardless of the substitution site. This implies that the crystal field surrounding europium(II) ions has non-axial symmetry. EPR spectral simulation suggests that the europium(II) ions preferentially occupy the site with the larger $|D|$ when they substitute for strontium ions. Comparison of the EPR spectra of $Sr_4Al_{14}O_{25}$: Eu and $SrAl_2O_4$: Eu,Dy phosphors shows that the $Sr_4Al_{14}O_{25}$: Eu is present as an impurity in the non-stoichiometric $SrAl_2O_4$: Eu,Dy when prepared with excess amounts of Al_2O_3. Such materials have been found to have long phosphorescent characteristics.

Introduction

There has been increasing interest in lanthanides in low symmetry sites of various types of materials such as glasses, powders, single crystals and thin films because of potential applications. However, the understanding of such low symmetry lanthanide sites by means of EPR spectroscopy lags far behind that of high symmetry ones. The large zero-field splittings, because of the low symmetry, cause the wave functions to mix with each other.[1] As a consequence the insufficiently high microwave energy (when compared with the zero-field splittings) yields complex spectra which are difficult to analyse utilising simple perturbation theory. Valainis *et al.*[2] studied the EPR spectra of gadolinium(III) and europium(II) doped in polycrystalline YAG : Sc, phosphorus oxynitride and $(Sr,Ba)_5(PO_4)_3$ at microwave frequencies of 4.6, 8.5, 9.5 and 10.5 GHz. However, simulation of the experimental spectra has not yet been successful. Also, Karthikeyani *et al.*[3] have recently reported complex X-band spectra of europium(II)-doped X-ray storage phosphor, but the interpretation is too speculative.

We have shown previously that high frequency EPR spectroscopy is a powerful tool to investigate low symmetry europium(II) sites for $CaAl_2O_4$: Eu,Nd,[4] $SrAl_2O_4$: Eu,Dy[4] and $BaAl_2O_4$: Eu.[5] All are powder phosphors with low crystallographic symmetry and belong to the space groups $P2_1/n$,[6] $P2_1$[7] and $P6_322$,[8] respectively. All the EPR spectra obtained can be interpreted based on their crystallographic data except for the non-stoichiometric $SrAl_2O_4$: Eu,Dy, which was prepared with an excess amount of Al_2O_3. Europium(II)-doped $SrAl_2O_4$ has interesting luminescent characteristics, decay of the 520 nm photoluminescence (PL) emission band was found to depend significantly upon the stoichiometry of the host and the co-doped impurities.[9–11] The experimental EPR spectrum[4] was simulated by assuming the presence of an extra site for the non-stoichiometric $SrAl_2O_4$: Eu,Dy. This was because the number of weak satellites appearing on both sides of the intense signal at about $g = 2$ was more than that found for the stoichiometric material. However, we were unable to explain this extra site. As a consequence we re-examined $Sr_4Al_{14}O_{25}$: Eu with an Al/Sr ratio 3.5 × larger than that of $SrAl_2O_4$, and have compared the results obtained with those for $SrAl_2O_4$: Eu,Dy.

Experimental

$Sr_4Al_{14}O_{25}$: Eu and $SrAl_2O_4$: Eu,Dy powder phosphors were prepared by calcining mixtures of $SrCO_3$, Al_2O_4 and Ln_2O_3 (Ln = Eu and Dy) in a reducing atmosphere either at 1300 °C together with B_2O_3 as a flux, or at 1400 °C without a flux as described elsewhere.[4,5] Formation of $Sr_4Al_{14}O_{25}$: Eu and $SrAl_2O_4$: Eu,Dy was checked by X-ray diffractometry and PL measurements (Figs. 1 and 2). High frequency (90 and 180 GHz) spectra were measured either at room temperature or at 145 K using a novel quasi-optical induction mode spectrometer that was designed and built at the University of St. Andrews, UK. A Fourier-transform Monte Carlo method[4,12] was used for the EPR spectral simulation. The basic powder pattern was obtained by sampling the spin-Hamiltonian in 1×10^6 directions of the unit sphere, and accumulating the

DOI: 10.1039/b004061o

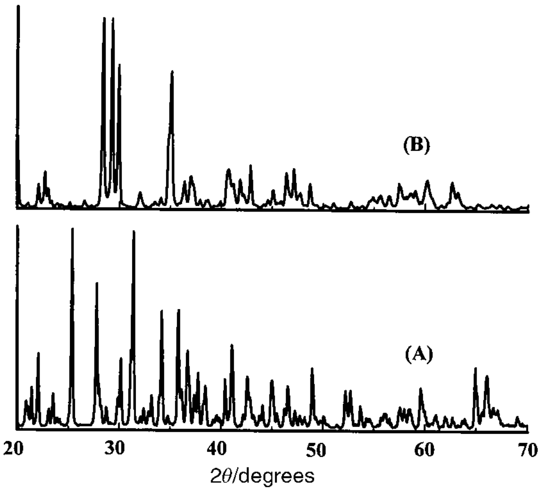

Fig. 1 X-Ray diffractograms of $Sr_4Al_{14}O_{25}$: Eu (A) and non-stoichiometric $SrAl_2O_4$: Eu,Dy (B) prepared by calcining a mixture of $SrCO_3$, Al_2O_3 and Ln_2O_3 (Ln = Eu and Dy) under a H_2/N_2 gas flow.

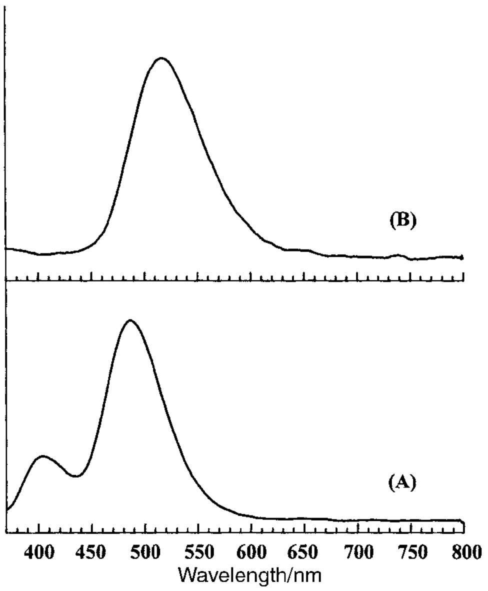

Fig. 2 Photoluminescence spectra of $Sr_4Al_{14}O_{25}$: Eu (A) and non-stoichiometric $SrAl_2O_{14}$: Eu,Dy (B) recorded at room temperature.

results in 1024 registers in linear relation to the magnetic field scan.

Results and discussion

Fig. 3 shows the 90 and 180 GHz EPR spectra of $Sr_4Al_{14}O_{25}$: Eu together with the simulated spectrum for 180 GHz. As can be seen in Fig. 3(A) and (B), the EPR spectra recorded at 90 and 180 GHz are fundamentally similar to each other with only a small difference in the intense central resonance at $g \cong 2$. At 90 GHz this resonance is split into a triplet, which is not the case at 180 GHz. This shows that the central resonance includes frequency dependent signals. From its crossover point this central resonance's g-value is calculated to be 1.988.

All the weak satellites observed on both sides of the intense signal are shoulders, but not divergences. In other words, they show absorption-like features, but not derivative shapes. The EPR due to europium(II) with an effective electron spin quantum number of $S = 7/2$ in non-cubic sites is expected to show seven fine structure transitions. The energies to second order are expressed as[13]

$$\begin{aligned}
E(M_S) = {} & GM_S + 1/2\{M_S^2 - 1/3S(S+1)\}\{D(3\cos^2\theta - 1) \\
& + 3E\sin^2\theta\cos 2\phi\} + 2M_S\{2M_S^2 + 1/4 - S(S+1)\} \\
& \{(D - E\cos 2\phi)^2\sin^2\theta\cos^2\theta + (E\sin 2\phi)^2\sin^2\theta\}/G_0 \\
& + M_S\{2S(S+1) - 2M_S^2 - 1\}\{\{D\sin^2\theta + E\cos 2\phi(1+\cos^2\theta)\}^2 \\
& + 4(E\cos\theta\sin 2\phi)^2\}/8G_0 \qquad (1)
\end{aligned}$$

in which G and G_0 are $g\beta H$ and hv_0 (β is the Bohr magneton, H is the applied magnetic field, h is Planck's constant and v_0 is the microwave frequency), respectively. M_S is the spin magnetic quantum number, D and E are the uniaxial and rhombic zero-field splitting parameters, respectively, and θ and ϕ are the Euler angles. From eqn. (1) it is suggested that for the powder pattern for a $^8S_{7/2}$ ion[4,12] divergences and shoulders should appear at around $|D|$, $2|D|$ and $3|D|$ positions and $2|D|$, $4|D|$ and $6|D|$ positions, respectively, away from the intense signal at $g = 2$ under axial symmetry of $E = 0$. When the symmetry is lowered, which means $0 < E \leqslant 1/3$, each divergence splits into a divergence and a shoulder. The magnetic fields where divergences appear should depend significantly upon the applied frequency. In contrast, the shoulders should merge into the signals at the $2|D|$, $4|D|$ and $6|D|$ positions under the extreme condition of $|E/D| = 1/3$, in which E is the rhombic zero-field splitting parameter. In this case therefore, only three

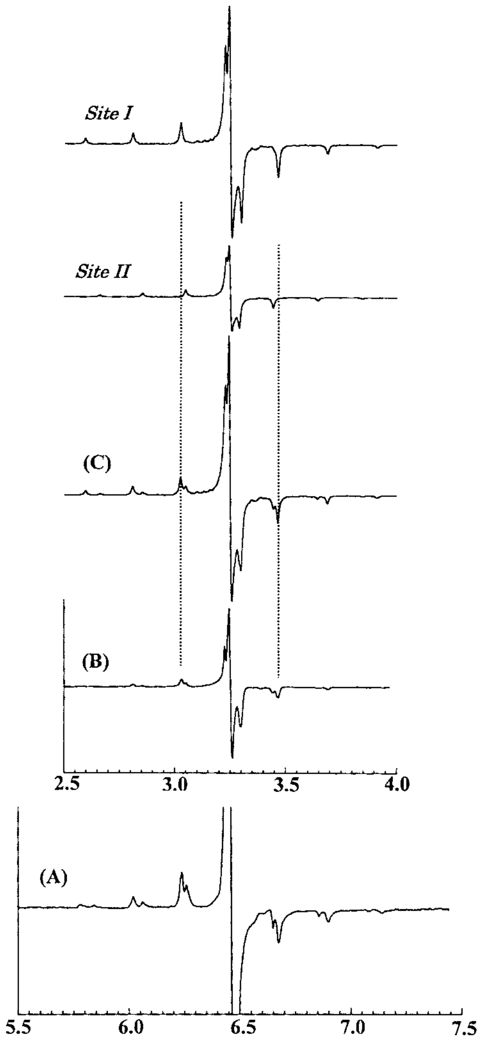

Fig. 3 EPR spectra of $Sr_4Al_{14}O_{25}$: Eu. (A) and (B) stand for the experimental spectra recorded at 180 GHz at 145 K and at 90 GHz at room temperature, respectively. (C) denotes the simulated spectrum at 90 GHz using the zero-field splitting parameters of $|D_{siteI}| = 0.102\ cm^{-1}$, $|E/D_{siteI}| = 1/3$ and $|D_{siteII}| = 0.092\ cm^{-1}$, $|E/D_{siteII}| = 1/3$, respectively. The intensity ratio of *siteI* and *siteII* is 3 : 1.

shoulders on both sides of the intense signal should be observed.

In Fig. 3(B) the observed EPR spectrum at 90 GHz has six shoulders on both sides of the triplet, which is twice as many satellites compared with those for a single site with $|E/D| = 1/3$. Thus there is the possibility that there are two different europium(II) sites with a $|E/D|$ ratio close to 1/3 present in $Sr_4Al_{14}O_{25}$. The other possibility is a single site with an intermediate value of $0 < |E/D| < 1/3$. However, spectral simulation excludes this latter possibility. At 90 GHz strong divergences appear next to the intense triplet at $g \cong 2$ when an $|E/D|$ of $\ll 1/3$ is assumed in the simulation in order to reproduce the six shoulders at the positions observed in the experimental spectrum. The shoulders which are split from the divergences have similar intensities to those at the $2|D|$, $4|D|$ and $6|D|$ positions. Therefore, two sets of $|D|$ values are estimated utilising the intervals between the shoulders at 3.04 and 2.8 T and between those at 3.05 and 2.85 T in the 90 GHz EPR spectrum.

The EPR spectral simulation was carried out assuming a Lorentzian lineshape with a peak-to-peak linewidth of 0.0070 T at 90 GHz. The spectrum obtained by overlapping the calculated spectra of two sets of zero-field splitting parameters of $|D| = 0.100$ and $0.0907\ \mathrm{cm^{-1}}$ with an intensity ratio of 3 : 1 (Fig. 3(C)) fits reasonably well with the experimental one (Fig. 3(B)), in which $|E/D|$ was a constant of 1/3. Consequently this implies that the europium(II) ions occupy two different sites. Also, the site with $|D| = 0.100\ \mathrm{cm^{-1}}$ occurs three times more than that with $|D| = 0.907\ \mathrm{cm^{-1}}$.

According to the XRD analysis of $Sr_4Al_{14}O_{25}$ powder by Minquan *et al.*[14] and Nadzhina *et al.*,[15] $Sr_4Al_{14}O_{25}$ belongs to the orthorhombic space group *Pmma* with $a = 24.765$ Å, $b = 8.478$ Å and $c = 4.882$ Å. The structure is built up of alternating planes consisting of AlO_6 octahedra and AlO_4 tetrahedra, and the strontium ions are in the cavities of the AlO_4 tetrahedra which interconnect them. The strontium sites are expressed as 4i.m. and 4j.m. using Wyckoff letters, which means that the two sites occur equally in the unit cell. In contrast, the EPR evidence for $Sr_4Al_{14}O_{25}$: Eu presented in this study suggests that one europium site occurs three times more than the other. How do we explain what this discrepancy is due to?

Smets *et al.*[16] observed two PL emission bands centred at 400 and 490 nm for $Sr_4Al_{14}O_{25}$: Eu with a large difference between their intensities. They interpreted this in terms of energy transfer arising because of the spectral overlap between the emission band of 400 nm and the excitation band of the 490 nm emission. The difference in PL intensity is due to europium(II) ions being preferentially substituted for strontium ions in the one site rather than the other, as well as the energy transfer, if one takes into account the EPR simulation in this study and the large difference in the mean Sr–O bond length between the two sites of 0.18 Å. This thesis is supported by the fact that a similar site preference was observed for $CaAl_2O_4$: Eu.[4] Also, it is deduced that sites with $|D|$ of 0.116 and $0.105\ \mathrm{cm^{-1}}$ are assigned to have mean Sr–O bond lengths of 2.74 and 2.56 Å, respectively.

Fig. 4 shows the 180 GHz EPR spectrum of $Sr_4Al_{14}O_{25}$: Eu together with that of $SrAl_2O_{14}$: Eu,Dy. The EPR spectrum of $Sr_4Al_{14}O_{25}$: Eu constitutes a part of non-stoichiometric $SrAl_2O_4$: Eu,Dy although it would appear that there is a difference in their *g*-values. The magnetic field was not calibrated for the respective EPR measurements because of the wide scan-width of 2.5 T. This may be the reason why this apparent difference in *g*-value was observed. However, because of this discrepancy the following discussion is limited to a consideration of the zero-field splitting parameters only.

All the satellites of $Sr_4Al_{14}O_{25}$: Eu appear at the satellite positions observed for non-stoichiometric $SrAl_2O_{14}$: Eu,Dy, but not for the stoichiometric material. In particular, quintets next to the intense resonance at $g \cong 2$ fit each other well. Overlapping the two simulated spectra for stoichiometric $SrAl_2O_4$: Eu,Dy and $Sr_4Al_{14}O_{25}$: Eu with an appropriate intensity ratio of 5 : 1 yields a spectrum with quintets on both sides of the intense signal (Fig. 5). This implies that the long phosphorescing non-stoichiometric $SrAl_2O_4$: Eu,Dy, prepared with a little excess of Al_2O_3 compared to $SrCO_3$, contains $Sr_4Al_{14}O_{25}$: Eu as an impurity.

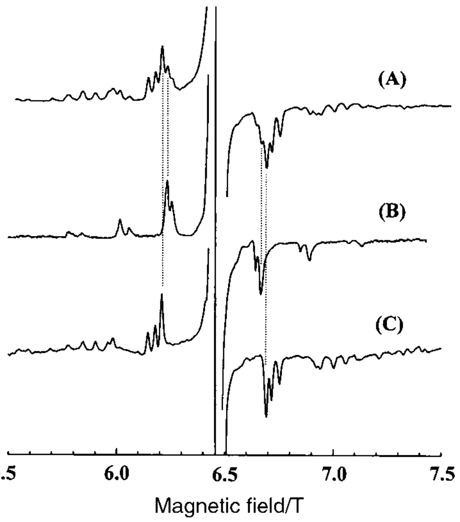

Fig. 4 A comparison of the 180 GHz EPR spectra of $Sr_4Al_{14}O_{25}$: Eu and $SrAl_2O_4$: Eu,Dy recorded at 145 K. (A), (B) and (C) stand for non-stoichiometric $SrAl_2O_{14}$: Eu,Dy, $Sr_4Al_{14}O_{25}$: Eu and stoichiometric $SrAl_2O_4$: Eu, respectively.

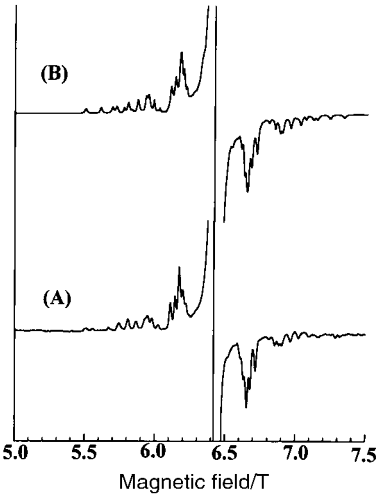

Fig. 5 High frequency EPR spectra of non-stoichiometric $SrAl_2O_{14}$: Eu,Dy. (A) and (B) stand for the experimental spectrum recorded at 178.652 GHz and the simulated one using the zero-field splitting parameters of stoichiometric $SrAl_2O_{14}$: Eu,Dy with $|D_{siteI}| = 0.142\ \mathrm{cm^{-1}}$, $|E/D_{siteI}| = 0.258$ and $|D_{siteII}| = 0.113\ \mathrm{cm^{-1}}$, $|E/D_{siteII}| = 0.306$, and of $Sr_4Al_{14}O_{25}$ with $|D_{siteI}| = 0.102\ \mathrm{cm^{-1}}$, $|E/D_{siteI}| = 1/3$ and $|D_{siteII}| = 0.092\ \mathrm{cm^{-1}}$, $|E/D_{siteII}| = 1/3$, respectively.

In our previous paper[4] we reported that non-stoichiometric $SrAl_2O_{14}$: Eu,Dy has three sites that are available for europium(II) ions, in contrast to two sites in stoichiometric $SrAl_2O_{14}$: Eu,Dy. The presence of this extra site was based on the EPR spectral simulation although there was a slight difference between the simulated and experimental spectra. The speculation was based on the fact that there is little indication of the formation of aluminates with different compositions in the XRD pattern (Fig. 1). For $Sr_4Al_{14}O_{25}$: Eu strong diffraction lines are observed at $2\theta = 25.4$ and $31.4°$, while for non-stoichiometric $SrAl_2O_{14}$: Eu,Dy no diffraction lines are observed. Also, the broad PL spectrum of non-stoichiometric

$SrAl_2O_4$: Eu,Dy is too unresolved to prove the presence of $Sr_4Al_{14}O_{25}$: Eu (Fig. 2). For this reason non-stoichiometry due to the Al/Sr ratio >2 should form vacancies somewhere in the $SrAl_2O_4$ tridymite structure, and that one of the three sites for europium(II) ions is related to these vacancies.

Conclusion

Europium(II) ions are in two low symmetry sites of $Sr_4Al_{14}O_{25}$: Eu with $|D| = 0.100$ and $0.0907\ cm^{-1}$, in which $|E/D|$ is 1/3 for both sites. Two different strontium sites occur equally in a unit cell of the host; europium(II) ions substitute in one strontium site in preference to the other. This is attributed to the large difference in the mean Sr–O bond length between these sites. From the comparison of the EPR spectra of $Sr_4Al_{14}O_{25}$: Eu and $SrAl_2O_{14}$: Eu,Dy it is clear that for non-stoichiometric $SrAl_2O_{14}$: Eu,Dy the signals assigned previously as an extra site are due to those of europium(II) in $Sr_4Al_{14}O_{25}$: Eu.

Acknowledgements

This work was supported by the Japan Society for the Promotion of Science through a grant-in-aid for the Scientific Research (A) No.12355030. K. K is greatly indebted to the British Council for the financial help to visit St. Andrews University for high frequency EPR measurements.

References

1 J. M. Baker, in *Electron Spin Resonance Vol. 13B*, ed. M. C. R. Symons, Royal Society of Chemistry, Cambridge, 1993, p. 131.
2 A. Valainis and L. Cugunovs, *Latv. J. Phys. Tech. Sci.*, 1993, **6**, 16.
3 A. Karthikeyani and R. Jagannathan, *J. Lumin.*, 2000, **86**, 79.
4 T. Nakamura, T. Matsuzawa, C. C. Rowlands, V. Beltran-Lopez, G. M. Smith and P. C. Riedi, *J. Chem. Soc., Faraday Trans.*, 1998, **94**, 3009.
5 T. Nakamura, K. Kaiya, N. Takahashi, T. Matsuzawa, C. C. Rowlands, V. Beltran-Lopez, G. M. Smith and P. C. Riedi, *Phys. Chem. Chem. Phys.*, 1999, **1**, 4011.
6 W. Hörker and H. K. Mükker-Buschbaum, *J. Inorg. Nucl. Chem.*, 1976, **38**, 1803.
7 A.-R. Von Schulze and Hk. Müller-Busschbaum, *Z. Anorg. Allg. Chem.*, 1981, **475**, 205.
8 S.-Y. Huang, R. Von Der Mühll, J. Ravez, J. P. Chaminade, P. Hagenmuller and M. Couzi, *J. Solid State Chem.*, 1994, **109**, 97.
9 T. Matsuzawa, Y. Aoki, N. Takeuchi and Y. Murayama, *J. Electrochem. Soc.*, 1996, **143**, 2670.
10 M. Ashida, K. Okamoto, I. Ozaki, H. Fukada, K. Ohomi, S. Tanaka, H. Kobayashi, M. Hayashi and M. Minamoto, *Proc. Int. Display Workshop '98, Kobe*, 1998, p. 597.
11 T. Nakazawa and T. Mochida, *J. Lumin.*, 1997, **72–74**, 236.
12 V. Beltran-Lopez, *Appl. Magn. Reson.*, 1996, **10**, 1.
13 J. R. Pilbrow, in *Transition Ion Electron Paramagnetic Resonance*, Clarendon Press, Oxford, 1990.
14 W. Minquan, D. Wang and L. Guanglie, *Mater. Sci. Eng. B*, 1998, **57**, 18.
15 T. N. Nadzhina, E. A. Pobedimskaya and N. V. Belov, *Kristallografiya*, 1980, **25**, 938.
16 B. Smets, J. Rutten, G. Hoeks and J. Verlijsdonk, *J. Electrochem. Soc.*, 1989, **136**, 2119.